THE ASTROPHYSICAL JOURNAL, 305:591–599, 1986 June 15

THE STELLAR POPULATION IN THE HALOS OF M31 AND M33

JEREMY MOULD
Palomar Observatory, California Institute of Technology

AND

JEROME KRISTIAN
Mount Wilson and Las Campanas Observatories, Carnegie Institution of Washington
Received 1985 May 24; accepted 1985 November 4

ABSTRACT

We present deep two-color (V and I) CCD photometry of stars in the halos of M31 and M33. The color-magnitude diagrams show the brightest 2 mag of the giant branches in the two galaxies. The M31 halo giant branch is very broad, indicating a large dispersion in metallicity, and the M33 halo giant branch is much narrower and less metal-rich; quantitative estimates for the mean values of [M/H] are -0.6 in M31 and -2.2 in M33. Comparison of the observed brightness of the tips of the giant branches with the calibration of Frogel, Cohen, and Persson give distance moduli of 24.4 ± 0.25 for M31 and 24.8 ± 0.3 for M33.

Subject headings: galaxies: individual — galaxies: stellar content

I. INTRODUCTION

Study of the stellar content of the foremost spiral galaxy in the Local Group has been confined almost entirely to the luminous objects of Population I. Fifty years of work on M31 has been summarized by van den Bergh (1968) and Hodge (1981); with the exception of studies in integrated light of the globular clusters, the investigation of Population II has not proceeded beyond the resolution of faint red stars in the central bulge by Baade (1944).

We know even less about Population II in M33. Indeed, since M33 is a pure disk system in the classic work of Freeman (1970) and de Vaucouleurs (1959) and since old star clusters are rare (Christian and Schommer 1983), one might even question the existence of Population II in this galaxy. More recently, Boulesteix *et al.* (1979) have isolated a small nuclear bulge in M33 with approximately 2% of the total luminosity.

The present study is a first look with modern detectors at the halos of these archetypal spiral galaxies. Fields were chosen several kiloparsecs from the centers of the galaxies, where photometry can be carried out without sophisticated treatment of crowding problems. The resultant color magnitude diagrams are compared with those of NGC 147, NGC 205 (Mould, Kristian, and Da Costa 1983, 1984, hereafter Papers I and II), and Galactic globular clusters.

II. PHOTOMETRY

The field studied in M31 is 7 kpc out on the minor axis in a southeast direction, centered on the cluster G298 (Sargent *et al.* 1977). The M33 halo field is in the same location relative to the center of that galaxy. The M33 field can be found just north of a bright star at ($1^h32^m26^s$, $+30°10'00''$, 1950). These fields were observed with the prime-focus universal extragalactic instrument (PFUEI; Gunn and Westphal 1981) at the prime focus of the Hale Telescope on the nights of 1983 October 29 and 30. The detector was an 800 × 800 pixel Texas Instruments CCD. Employing the same filters used in Papers I and II, on the first night we obtained nine 300 s exposures on each field in both V and I. On the second night these were supplemented with six 300 s R frames and eight 450 s V frames of the M31 field. A number of short exposures of these fields and of standard fields (Paper I) were also obtained. The seeing ranged between 1''.3 and 1''.6 FWHM.

The pictures were debiased, flattened with dome flats, and stacked. The two nights' V frames were stacked separately. The intensities of all uncrowded stellar images within a central 500 pixel square area was measured in two stages. First, the intensities within 2 pixels (0''.83) of the star centers were measured. These partial intensities were then converted to total intensities by comparison with the radial intensity profiles of the brightest unsaturated stars. Crowding, and perhaps variations of the instrumental point spread function, make these total intensity corrections uncertain by 0.05 mag in I and $V-I$ for M31. Poorer seeing and a lack of bright stars to properly calibrate the corrections raises this uncertainty to 0.1 mag in M33. This represents the limiting external accuracy of the current data for bright stars in these fields. *Repeatability* between the two nights' V frames is better than this, starting at 0.02 mag rms at $V = 19$–21.5, 0.07 mag at $V = 21.5$–22.5, 0.11 mag at $V = 22.5$–23.5, and reaching 0.2–0.3 mag from $V = 23$–24. Very tight transformations to standard star sequences in NGC 7790 and NGC 2419 ensure that we are exactly on the system of Paper I. Standardization uncertainties are negligible compared with the aperture correction uncertainty mentioned above.

The resultant colors and magnitudes on the Cousins (1976) system are given in Table 1. Column (1) is a running star number, which generally permits identification of the star on Figure 1 (plate 8). Columns (2) and (3) give the pixel coordinates. Columns (4) and (5) give the I magnitude and $V-I$ color respectively. The rms uncertainty in the V magnitude is given in column (6) in units of 0.01 mag. Stars brighter than $I = 23$ whose V magnitudes differed between October 29 and 30 by more than 0.3 mag are flagged with asterisks in column (6). These stars might be real variables. Table 2 contains no column (6), because only single V measurements are available. All the program stars are identified in Figures 1 and 2 (plate 9).

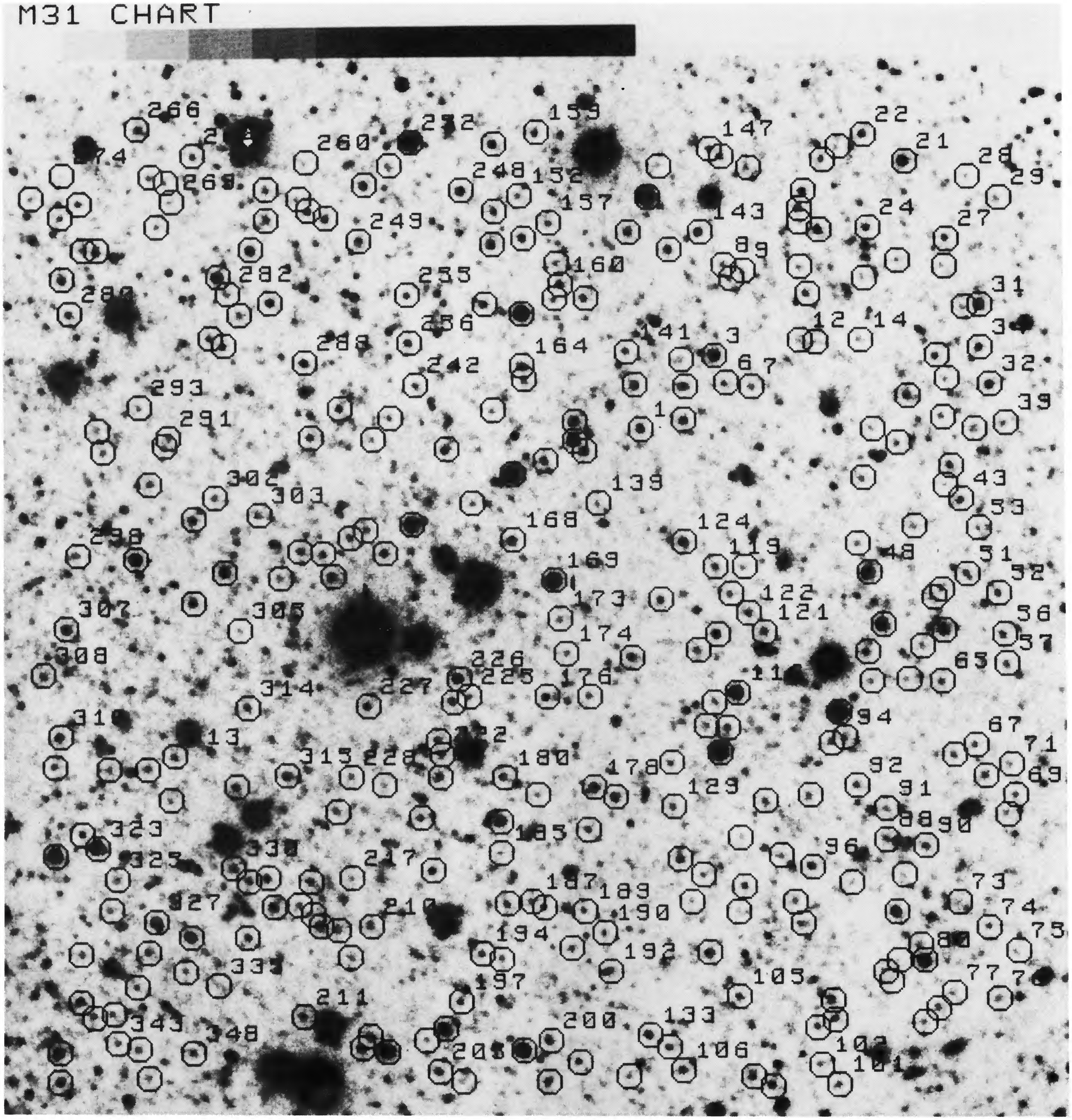

FIG. 1.—The central 500 × 500 pixels of the M31 halo field. This exposure represents a total of 30 minutes through a red filter. North is down and east to the right. Each bar of the grey scale at the top is 1.4 arcsec. Uncrowded stars are numbered above and to the right of their identifying circle. Stars without numbers can be identified from the pixel coordinates in Table 1. The cluster G298 is northeast of star 168.

MOULD AND KRISTIAN (*see* page 591)

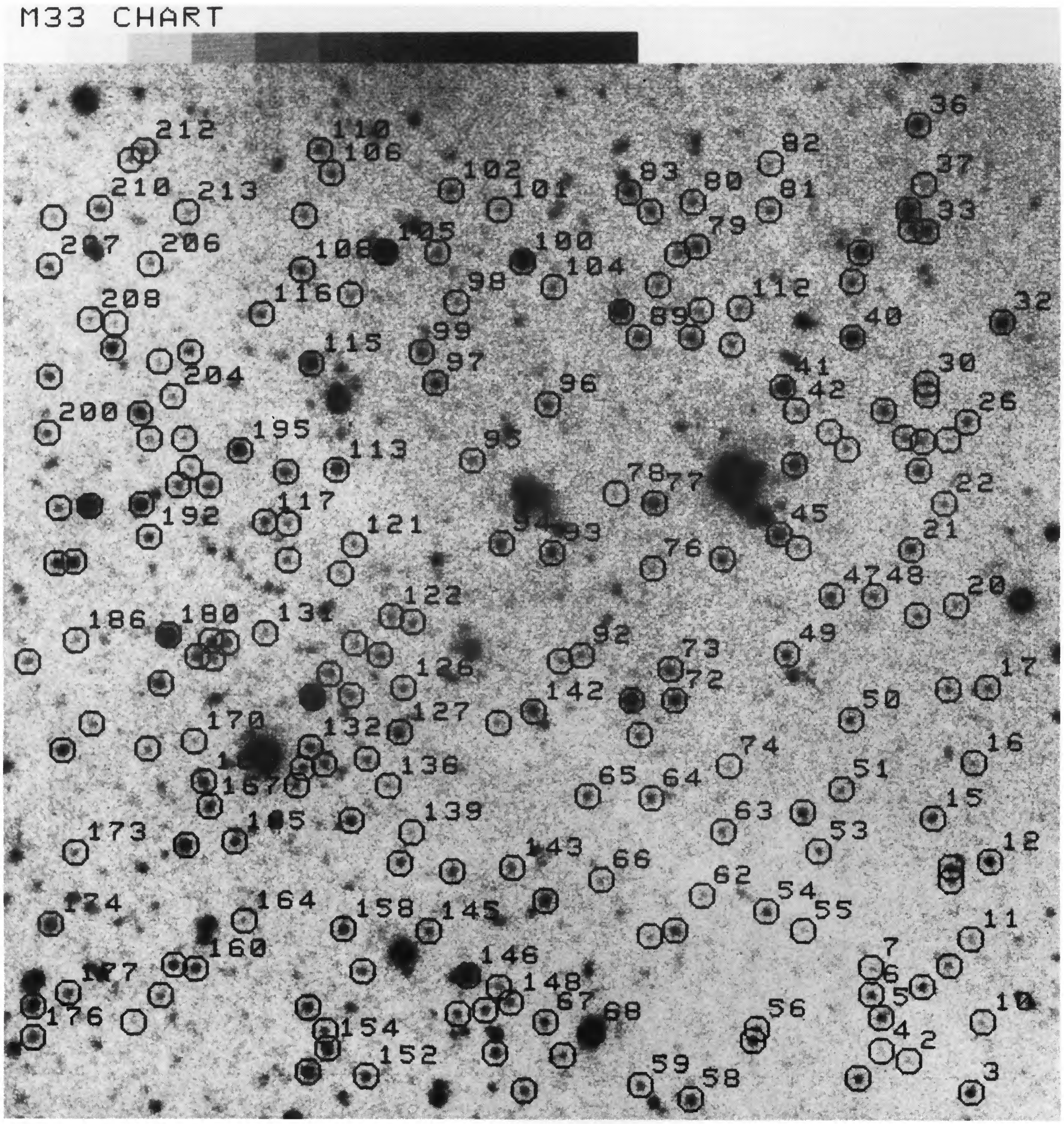

FIG. 2.—The central 500 × 500 pixels of the M33 halo field. The scale and orientation of the 30 minute infrared frame are the same as for Fig. 1. Stars are identified in Table 2.

MOULD AND KRISTIAN (*see* page 591)

TABLE 1

PHOTOMETRY IN M31

	x	y	I	V-I	
(1)	(2)	(3)	(4)	(5)	(6)
1	462	487	20.99	1.35	[2]
2	484	492	20.90	1.54	[8]
3	500	525	19.68	2.01	[1]
4	483	523	21.10	2.18	**
5	485	509	20.94	2.15	[7]
6	506	511	21.42	1.56	**
7	519	509	22.02	1.22	[6]
8	505	572	22.38	1.39	[12]
9	515	569	22.69	1.01	[10]
10	509	565	22.25	1.46	[12]
11	548	557	21.26	1.79	[1]
12	544	533	21.47	2.58	[6]
13	552	532	21.63	2.74	[25]
14	575	533	22.77	1.20	[25]
15	544	571	22.31	1.32	[3]
16	554	590	20.54	2.00	[3]
17	544	594	22.42	1.76	[21]
18	544	601	20.87	1.94	[3]
19	546	610	20.88	2.06	[1]
20	556	626	21.78	1.45	[2]
21	598	625	19.40	2.84	[5]
22	577	639	21.17	1.52	[3]
23	564	633	23.06	1.62	[50]
24	579	591	21.04	2.03	[5]
25	577	565	22.20	1.87	[25]
26	594	574	22.64	1.31	[11]
27	619	585	21.54	1.68	[12]
28	630	617	21.50	3.31	[14]
29	646	606	20.96	3.50	[6]
30	618	571	22.37	1.67	[12]
31	636	551	19.95	1.86	[2]
32	641	510	20.80	1.53	[5]
33	628	550	21.58	2.98	[33]
34	636	529	20.89	2.08	[7]
35	614	525	21.24	1.94	[6]
36	619	513	22.16	2.17	[10]
37	599	504	20.37	2.70	[5]
38	617	493	22.41	1.08	[8]
39	649	490	21.97	1.64	[10]
40	633	487	22.03	1.52	[5]
41	621	468	21.35	1.72	[5]
42	618	458	22.88	1.69	[31]
43	626	451	20.95	2.29	[8]
44	602	437	22.32	1.30	[5]
45	594	480	21.53	2.09	[5]
46	581	487	21.72	2.58	[14]
47	576	462	21.87	1.66	[9]
48	579	413	18.87	2.95	[3]
49	573	428	22.08	1.49	[8]
50	612	400	20.99	2.86	[32]
51	629	412	21.34	1.74	[4]
52	645	402	21.51	1.34	[7]
53	635	436	22.06	1.61	[18]
54	616	404	21.74	1.46	[14]
55	617	383	19.73	2.04	[4]
56	648	381	21.02	2.06	[5]
57	649	366	21.35	2.13	[15]
58	606	375	20.97	2.88	[10]
59	586	386	19.64	0.89	[3]
61	578	372	21.11	1.67	[8]
62	563	341	18.00	1.88	[3]
63	580	357	21.85	1.84	[17]
64	599	358	22.61	1.42	[19]
65	616	357	21.75	1.36	[5]
66	622	319	21.68	1.48	[8]
67	633	324	21.83	1.38	[4]
68	638	308	20.97	2.25	[11]
69	653	298	21.99	1.43	[4]
71	651	314	22.49	1.39	[13]
72	649	288	21.75	1.94	[4]
73	624	243	21.36	2.10	[12]
74	639	230	21.79	1.84	[13]
75	654	218	22.77	0.96	[8]
76	644	193	20.93	2.78	[17]
77	621	196	22.04	1.81	[8]
78	613	188	20.82	2.64	[5]
80	606	213	19.23	1.94	[5]
81	604	221	22.13	1.15	[16]
82	606	181	22.22	0.30	**
83	589	202	21.46	2.73	[25]
84	586	207	21.82	2.17	[10]
85	593	213	22.69	2.11	[73]
86	592	238	20.33	1.95	[1]
87	569	253	21.37	3.39	[12]
88	587	275	21.02	1.03	[5]
89	596	257	21.75	3.49	[91]
90	607	272	21.40	1.45	[5]
91	587	291	21.83	2.13	[11]
92	572	303	21.04	2.35	[5]
93	559	325	21.59	1.83	[4]
94	566	328	21.20	2.40	[6]
95	548	298	21.80	1.70	[7]
96	549	261	21.15	1.42	[1]
98	559	192	21.13	1.40	[5]
99	551	178	21.68	1.76	[3]
100	560	182	21.52	1.35	[3]
101	562	149	20.91	2.92	[11]
102	553	159	22.11	1.34	[11]
103	528	148	21.04	1.89	[3]
104	518	153	21.37	1.51	[3]
105	511	194	20.83	3.00	[9]
106	482	156	20.95	2.16	[5]
107	496	217	20.84	2.15	[11]
108	511	238	21.09	4.45	[28]
109	544	232	21.80	1.66	[10]
110	540	243	22.23	1.30	[11]
111	514	251	21.71	1.46	[2]
112	512	276	22.78	1.32	[9]
113	525	295	20.53	3.31	[20]
114	533	267	22.10	1.44	[7]
115	502	320	18.34	1.00	[1]
116	511	351	19.23	1.48	[2]
117	491	373	20.36	3.87	[15]
118	501	381	20.67	1.53	[2]
119	500	416	21.59	1.22	[8]
120	508	402	21.63	1.81	[4]
121	525	382	20.34	2.96	[10]
122	517	392	21.37	1.60	[7]
123	515	416	22.57	1.11	[11]
124	484	429	20.57	1.85	[1]
125	472	399	20.99	2.11	[3]
126	495	334	21.44	2.80	[14]
127	499	346	21.36	2.80	[4]
128	477	315	21.56	2.06	[11]
129	478	292	22.07	1.24	[5]
130	481	265	20.83	2.02	[6]
131	493	257	21.87	2.17	[2]
132	487	243	22.71	1.68	[9]
133	465	174	21.03	1.44	[6]
134	475	168	21.59	1.45	[10]
135	454	153	22.22	2.00	[22]
137	506	333	21.78	1.32	[10]
138	457	369	20.94	1.94	[2]
139	440	449	21.57	2.95	[12]
140	459	510	20.91	1.39	[11]
141	455	527	21.78	1.60	[0]
142	477	580	20.82	2.09	[9]
143	493	589	20.92	1.66	[3]
145	466	607	18.19	1.62	[1]
146	472	623	23.13	0.95	[12]
147	498	632	21.51	1.91	[7]
148	518	622	21.59	2.40	[16]
149	504	628	21.76	1.29	[5]
150	456	589	20.79	2.23	[7]
152	400	608	21.25	2.25	[9]
153	387	600	20.93	2.88	[11]
154	387	635	20.98	1.79	[11]
155	386	583	20.78	1.98	[8]
156	402	586	20.93	2.17	[7]
157	415	594	21.87	1.57	[7]
158	419	573	21.44	2.23	[17]
159	409	641	21.65	1.45	[8]
160	421	562	21.05	1.95	[6]
161	418	555	22.24	1.51	[22]
162	434	555	21.37	1.62	[7]
163	401	547	19.84	1.02	[5]
164	401	520	20.91	1.82	[4]
165	402	513	21.36	2.24	[7]
166	428	481	19.80	0.98	[5]
167	433	476	20.71	1.80	[8]
168	396	430	20.68	1.91	[5]
169	417	409	18.56	1.64	[3]
171	413	471	20.77	2.31	[10]
172	428	491	20.61	1.65	[3]
173	420	389	22.43	1.35	[18]
174	423	371	22.02	2.26	[19]
175	435	349	21.06	3.26	[15]
176	413	349	21.18	1.93	[6]
178	437	302	20.12	2.22	[3]
179	408	298	21.59	2.80	[25]
180	391	307	21.44	1.81	[7]
181	389	284	20.59	1.76	[0]
182	434	280	21.77	1.51	**
184	448	297	20.88	1.86	[6]
185	389	268	22.45	2.12	[23]
186	392	242	20.89	2.73	[5]
187	405	243	21.17	2.66	[9]
188	411	240	21.64	1.60	[11]
189	432	238	21.95	2.02	[15]
190	442	227	21.12	3.19	[13]
191	425	219	22.13	1.53	[4]
192	445	207	20.73	2.30	[4]
193	389	213	21.94	2.04	[33]
194	379	216	21.58	1.76	[8]
197	368	191	20.97	2.81	[7]
198	360	177	18.99	2.32	[2]
199	400	166	18.85	1.38	[2]
200	414	171	21.09	1.57	[10]
201	429	160	21.60	1.90	[10]
202	413	150	21.56	1.34	[1]
203	369	150	21.43	1.97	[8]
204	350	171	22.58	1.45	[18]
205	357	155	21.13	2.01	[1]
206	330	165	20.46	1.00	[1]
207	317	167	20.89	1.70	[1]
208	321	173	21.12	1.85	[10]
209	311	214	21.29	2.96	[15]
210	322	230	20.59	2.89	[3]
211	287	183	21.29	1.46	**
212	296	230	19.93	3.08	[7]
213	292	236	21.95	2.16	[7]
214	285	241	22.20	1.24	[14]
215	291	253	21.44	1.46	[4]
216	305	228	21.35	1.92	[11]
217	312	255	22.42	1.99	[5]
218	305	289	21.96	1.19	[7]
219	329	303	21.45	3.19	[23]
220	358	307	21.24	1.76	[3]
222	359	319	21.69	1.62	**
223	357	326	21.72	1.53	[10]
224	365	346	21.41	1.71	[4]
225	373	349	22.31	1.39	[3]
226	368	358	20.70	0.96	[3]
227	321	344	21.38	1.61	[2]
228	312	307	21.86	1.79	[11]
229	348	286	21.69	1.78	[2]
230	354	259	21.45	1.48	[7]
232	344	438	20.14	1.72	[3]
233	330	423	21.38	1.71	[5]
234	320	435	21.83	1.45	[9]
236	303	411	20.69	2.24	[2]
237	298	423	21.48	1.98	**
238	286	424	21.04	2.30	[2]
239	312	431	21.76	1.60	[2]
240	324	482	22.13	3.11	[51]
241	333	493	21.61	2.53	[21]
242	346	510	21.18	2.75	[6]

TABLE 1—*Continued*

(1)	x (2)	y (3)	I (4)	V-I (5)	(6)	(1)	x (2)	y (3)	I (4)	V-I (5)	(6)
243	362	477	21.24	1.62	[5]	296	208	459	20.94	2.78	[3]
244	375	449	22.29	2.25	[16]	298	171	422	21.78	1.97	**
245	396	464	17.87	2.06	[5]	299	201	420	19.70	1.32	[1]
246	386	497	21.18	3.59	[16]	300	247	413	20.01	2.31	[5]
247	382	552	21.01	1.92	[13]	301	231	441	20.67	2.06	[1]
248	370	611	19.93	3.23	[8]	302	242	452	21.75	2.00	[10]
249	317	585	20.03	3.71	[17]	303	265	443	21.40	1.83	[4]
250	320	614	21.16	1.59	[9]	304	276	410	22.16	1.84	[10]
251	333	624	20.66	4.17	[18]	305	255	383	22.34	2.19	[18]
252	344	636	18.13	2.15	[5]	306	231	397	21.06	1.55	[3]
255	342	557	21.64	2.05	[1]	307	165	384	20.84	1.38	[3]
256	343	532	20.75	2.51	[7]	308	153	360	21.55	1.94	[11]
257	300	597	21.15	1.99	[13]	310	162	328	21.03	1.76	[8]
258	291	601	21.27	1.87	[8]	313	221	318	21.68	1.35	[6]
259	286	607	21.39	2.66	[9]	314	259	343	21.56	1.80	[15]
260	290	626	22.06	2.76	[24]	315	279	308	21.09	1.73	[6]
261	269	612	21.10	3.09	[15]	317	219	295	21.83	2.38	[11]
262	261	581	19.91	2.88	[4]	318	207	311	21.62	1.61	[4]
263	269	596	21.51	1.56	[3]	319	187	311	21.35	3.24	[31]
264	231	630	21.05	2.97	[16]	320	159	312	21.76	2.04	[16]
266	202	644	21.06	2.16	[6]	322	159	266	19.03	1.24	[3]
267	209	619	22.16	1.33	[11]	323	181	270	19.53	0.82	[1]
268	217	616	22.51	1.51	[23]	324	173	277	21.46	1.98	[3]
269	220	606	22.75	1.63	[10]	325	191	254	22.16	1.71	[18]
270	212	593	22.09	2.34	[51]	326	188	238	22.49	1.63	[8]
272	172	605	21.87	1.67	[19]	327	211	232	19.95	1.44	[2]
274	163	620	21.91	2.21	[17]	328	229	224	20.21	1.08	[1]
275	162	598	20.56	3.50	[48]	329	253	302	20.57	2.42	[6]
276	147	608	21.38	3.83	[41]	330	251	260	20.97	2.14	[4]
277	174	581	21.39	2.34	[11]	331	269	255	21.08	1.81	[3]
278	181	581	21.37	1.33	[7]	332	272	240	20.81	1.50	[3]
279	163	566	20.57	2.39	[6]	333	258	224	21.53	1.29	[3]
280	167	548	21.66	1.56	[7]	334	259	253	21.39	1.56	[8]
281	244	567	20.29	1.47	[2]	335	243	199	21.60	3.17	[31]
282	249	558	22.23	1.51	[19]	336	226	206	21.98	2.34	[8]
283	271	553	20.95	1.67	[4]	337	201	198	21.76	2.37	[6]
284	255	547	22.08	1.20	**	338	207	216	21.45	1.97	[3]
285	240	535	21.51	1.90	[5]	339	172	215	22.24	1.30	[10]
286	247	531	21.45	1.69	[3]	340	172	190	21.15	1.59	[4]
288	289	522	20.69	2.09	[8]	341	179	182	21.74	1.99	**
289	307	498	21.46	1.85	[6]	342	189	184	22.01	1.84	[10]
290	292	483	21.75	1.33	[2]	343	191	169	21.90	2.11	[15]
291	218	483	22.19	1.49	[8]	344	202	166	21.84	1.67	[5]
292	216	479	22.16	1.48	[11]	345	161	164	19.98	2.44	[2]
293	203	499	22.68	1.25	[12]	346	161	149	20.30	2.85	[2]
294	181	487	21.42	3.36	[17]	347	207	151	22.23	1.65	[18]
295	184	476	22.18	1.47	[1]	348	230	164	21.73	1.50	[7]

III. CHEMICAL COMPOSITION

Color-magnitude diagrams for the M31 and M33 halo fields are shown in Figures 3 and 4. Interpretation of these diagrams by comparison with those of globular clusters requires knowledge of the Galactic reddening. We adopt the estimates by Burstein and Heiles (1984), based primarily on H I column densities, of $A_B = 0.31$ mag for M31 and 0.18 mag for M33. These fields are sufficiently far from the planes of their respective galaxies to be free from internal reddening according to the H I maps of Cram, Roberts, and Whitehurst (1980) and Newton (1980).

In M31 the standard reddening ratios lead to $E(V - I) = 0.10$ and $A_I = 0.14$ mag. The lines in Figure 3 are the giant branches for M92 and 47 Tuc, corrected for these absorption values and for a distance modulus for M31 of $(m - M)_0 = 24.4$. This is the corrected Sandage and Tammann (1976) value used in Paper I. Figure 3 clearly shows the brightest 2 mag in luminosity of the M31 halo giant branch. Since the errors in $V - I$ are less than 0.2 mag for $V > 24$ ($I > 22.5$), the broadness of the M31 giant branch is real, indicating (if we assume that the stars are old) a large metallicity dispersion. From the mean value of $\langle V - I \rangle_0 = 1.68$ at $M_I = -3$; we estimate a mean metallicity of $\langle [M/H] \rangle > -0.8$ in the M31 field. This inequality is strengthened by the existence of a luminosity cutoff at $V \approx 24.5$ in the present data, and also by uncorrected contamination of the sample by foreground stars. Correction for these effects is expected to be small, however, since the distribution in color at constant magnitude in Figure 3 has a long, but sparse, tail, and foreground stars are only slightly bluer in the mean than M31 halo stars (see Paper II). If we ignore these effects and extrapolate the ($V - I$, $[M/H]$) calibration of Paper I, using Yale tracks as a guide (Ciardullo and Demarque 1977), we arrive at an estimate of -0.6 for $\langle [M/H] \rangle$ for the M31 field. The formal value of the color dispersion at $M_I = -3$ is $\sigma(V - I) = 0.55$ mag. Because of incompleteness in V, this is strictly a lower limit. We will

1986ApJ...305..591M

TABLE 2

PHOTOMETRY IN M33

	x	y	I	V-I		x	y	I	V-I		x	y	I	V-I		x	y	I	V-I
(1)	(2)	(3)	(4)	(5)	(1)	(2)	(3)	(4)	(5)	(1)	(2)	(3)	(4)	(5)	(1)	(2)	(3)	(4)	(5)
1	578	160	21.35	1.21	55	550	236	22.95	0.96	109	317	565	22.38	1.52	162	219	201	21.98	1.09
2	604	169	22.64	1.05	56	526	185	21.95	1.36	110	301	640	21.42	1.80	163	205	187	23.12	0.20
3	636	153	21.07	1.33	57	524	179	21.05	1.07	111	514	539	21.96	1.20	164	262	240	22.66	1.06
4	590	174	23.31	0.30	58	492	149	21.04	0.85	112	518	558	22.22	1.39	165	257	281	21.08	1.70
5	590	191	21.20	1.32	59	466	156	21.55	1.59	113	310	474	20.28	3.11	166	232	279	19.99	1.22
6	585	203	21.43	1.32	60	471	233	22.41	1.22	114	284	473	21.27	0.77	167	244	299	21.15	-0.08
7	585	217	22.50	1.19	61	484	236	21.05	1.68	115	297	529	19.75	1.04	168	241	312	20.79	-0.78
8	611	207	21.24	2.86	62	498	254	22.56	0.94	116	271	555	21.62	1.44	169	241	312	20.79	-0.78
9	625	218	21.84	1.13	63	509	287	22.16	1.24	117	273	447	21.36	1.38	170	236	333	22.80	1.23
10	642	189	22.43	1.00	64	472	304	21.43	1.61	118	285	446	22.17	1.27	171	212	329	22.13	1.21
11	636	232	22.63	1.38	65	439	305	21.76	1.79	119	285	427	21.93	1.28	172	168	328	20.53	2.41
12	646	272	20.93	3.64	66	446	262	22.63	1.50	120	312	420	22.60	1.97	173	175	275	22.04	1.39
13	626	269	21.10	1.62	67	417	188	21.18	1.61	121	319	435	22.41	1.05	174	162	238	20.23	2.77
14	626	262	21.85	1.11	68	441	183	18.52	1.47	122	338	398	21.99	1.50	175	153	195	20.24	2.18
15	617	294	21.36	1.30	69	426	171	21.93	1.41	123	349	395	21.77	1.30	176	153	179	21.58	1.22
16	638	323	22.56	1.15	70	466	337	21.93	1.07	124	332	378	21.57	0.84	177	171	202	21.42	1.44
17	645	362	21.64	1.18	71	462	355	19.56	0.88	125	319	384	22.38	0.95	178	183	342	22.14	1.31
18	625	361	21.98	1.72	72	484	355	20.57	2.19	126	344	361	22.05	1.35	179	219	363	20.68	2.50
19	609	399	21.93	1.44	73	482	371	21.17	1.81	127	342	338	20.72	1.60	180	223	388	18.61	2.76
20	629	404	22.41	1.37	74	512	321	23.12	0.28	128	297	356	17.80	2.27	181	245	385	21.16	1.47
21	606	433	21.03	0.88	75	509	428	21.37	1.60	129	317	357	21.78	1.40	182	253	384	21.16	1.61
22	623	457	22.16	1.33	76	473	423	22.82	1.36	130	306	368	21.51	1.79	183	238	377	21.16	1.62
23	610	474	20.82	1.20	77	474	457	20.51	0.43	131	273	389	22.44	1.43	184	246	376	21.99	1.31
24	612	489	21.84	1.12	78	454	462	22.97	2.35	132	296	330	21.35	0.73	185	150	374	21.90	1.34
25	625	490	22.85	0.72	79	496	590	21.12	1.23	133	292	319	21.62	1.25	186	175	385	22.46	1.13
26	635	499	21.49	1.41	80	494	613	21.81	1.28	134	303	321	21.44	1.22	187	165	425	20.84	1.85
27	603	491	21.93	1.40	81	533	609	21.76	1.04	135	325	324	21.93	1.49	188	174	426	20.49	1.25
28	573	485	22.20	1.25	82	534	633	22.59	0.84	136	336	310	22.38	1.18	189	166	454	21.65	1.78
29	592	505	21.32	2.10	83	461	618	20.45	1.93	137	317	292	20.95	1.34	190	182	455	18.18	2.49
30	614	519	21.92	1.26	84	472	608	21.34	1.27	138	342	270	21.37	1.10	191	209	456	19.68	0.73
31	614	513	22.24	1.58	85	486	586	21.79	1.25	139	348	286	22.74	1.22	192	213	439	21.07	1.60
32	653	551	20.38	3.06	86	476	570	22.20	1.02	140	369	266	21.57	0.82	193	228	466	21.58	1.14
33	614	598	20.66	2.57	87	498	557	22.11	1.05	141	393	343	22.37	1.84	194	244	466	21.45	1.23
34	606	599	21.59	1.28	88	493	543	21.25	2.08	142	411	349	20.98	1.38	195	260	484	19.84	2.79
35	605	609	20.54	1.24	89	466	543	21.27	1.27	143	400	268	21.86	1.36	196	234	475	22.64	1.15
36	610	653	20.68	0.71	90	457	556	19.41	0.71	144	417	251	20.42	2.83	197	231	490	22.51	1.03
37	613	622	22.52	1.90	91	425	375	22.09	1.40	145	357	235	21.60	1.39	198	213	490	22.26	1.33
38	580	587	20.05	2.66	92	436	378	22.03	1.06	146	377	212	19.39	1.46	199	208	503	20.49	2.50
39	576	572	21.70	1.19	93	421	431	20.96	2.28	147	393	206	22.00	1.24	200	160	493	21.56	3.15
40	576	543	19.81	0.81	94	395	436	21.28	1.16	148	399	198	21.64	0.97	201	161	522	21.16	2.74
41	540	517	20.07	1.28	95	380	479	22.03	1.41	149	386	194	21.51	1.49	202	194	537	20.36	1.39
42	547	505	22.39	0.78	96	419	508	21.45	1.63	150	391	172	21.04	1.41	203	234	535	21.32	1.57
43	564	494	22.54	1.05	97	361	519	20.93	2.28	151	406	153	21.44	1.48	204	225	512	22.58	1.35
44	546	477	20.52	2.28	98	372	561	22.56	2.51	152	325	160	21.15	1.47	205	218	530	22.87	1.22
45	538	441	20.26	2.69	99	354	535	21.28	1.72	153	295	162	20.30	1.65	206	213	581	22.13	1.15
46	548	434	22.54	1.10	100	406	582	19.14	1.62	154	305	174	20.43	0.58	207	161	580	21.49	1.42
47	565	409	21.11	1.17	101	394	609	22.57	1.26	155	304	183	21.62	1.48	208	182	552	22.40	1.10
48	587	409	21.72	0.99	102	369	619	21.57	2.14	156	295	195	21.02	1.39	209	195	550	23.07	0.70
49	542	379	21.05	1.51	103	362	587	21.92	2.79	157	323	214	21.67	3.00	210	187	610	21.28	1.40
50	575	345	21.43	1.32	104	422	569	22.02	1.37	158	313	236	20.83	1.83	211	203	635	22.01	1.22
51	570	309	22.07	0.82	105	335	587	18.21	3.02	159	372	192	21.61	1.31	212	210	640	21.64	1.28
52	550	297	21.07	1.46	106	307	628	21.71	1.45	160	237	215	21.05	1.78	213	232	608	22.55	0.80
53	558	277	21.81	1.33	107	293	606	21.98	1.32	161	226	217	20.95	2.02	214	163	605	22.59	1.49
54	531	246	21.39	1.57	108	292	578	21.37	1.57						215	289	310	21.75	1.13

address in a future paper how this estimate can be corrected and converted to a metallicity dispersion σ_z. Suffice it to say for the present that this color dispersion is the largest of the fields studied to date in M31 and its companions, just as the mean metallicity $\langle Z \rangle$ is larger than that of NGC 205 and NGC 147. A correlation between σ_z and $\langle Z \rangle$ is predicted by chemical enrichment models under a wide range of assumptions (Mould 1984).

With this high value of the mean metallicity one might wonder if the results have been affected by contamination from the disk of the galaxy. The disk to bulge ratio in this field can be estimated from surface photometry of M31 by de Vaucouleurs (1958). Extrapolation of his Figure 10 yields a blue spheroidal surface brightness of 26.2 mag s^{-2} in the field. Extrapolation of his major axis profile gives a disk surface brightness of 30.8 mag s^{-2}. The disk to bulge ratio is therefore 1.4%. This is an upper limit, as van der Kruit and Searle (1983) have shown that disks have "edges." i.e., a maximum radius of 4–5 scale lengths. The case for M33 is not quite so clear cut. The line of sight grazes the edge of the disk, which is warped, and lies somewhere between 35′ and 40′ from the center of the galaxy (de Vaucouleurs 1959).

For M33 we adopt $E(V - I) = 0.06$, $A_I - 0.08$ and $(m - M_0) = 24.8$. The distance modulus is again from Sandage

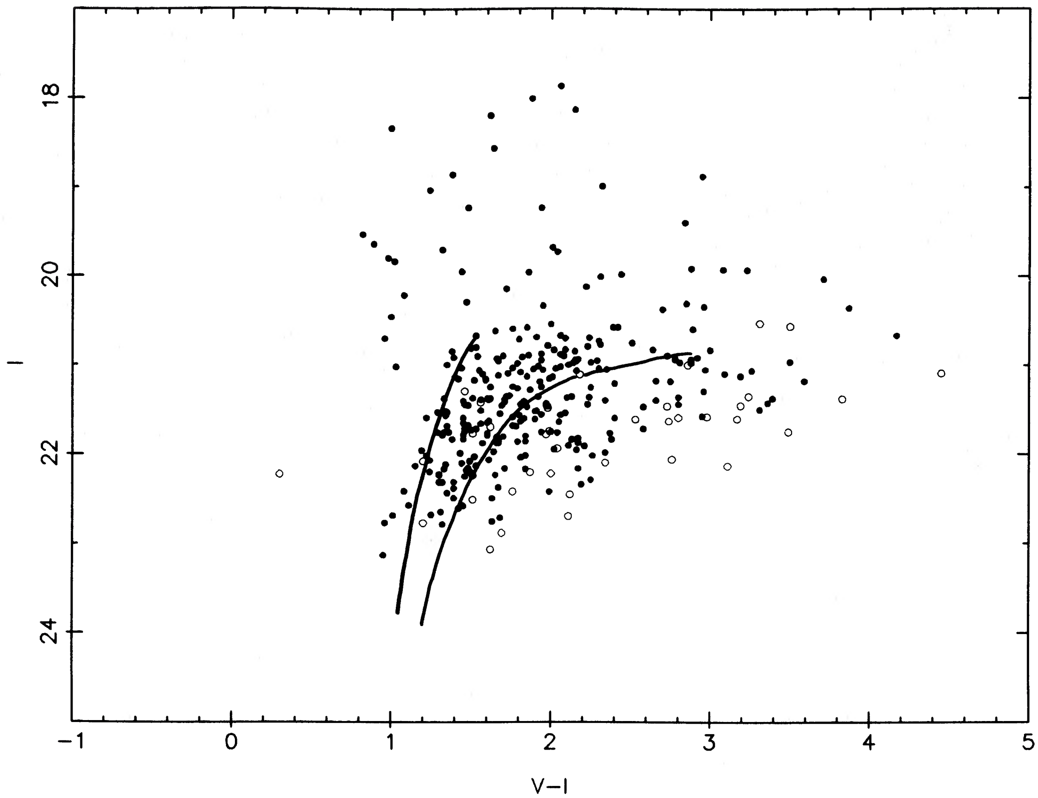

FIG. 3.—Color-magnitude diagram of the M31 halo field. Giant branches for M92 (*blue side*) and 47 Tuc (*red side*) are superposed at the adopted distance and reddening of M31. Open circles denote stars whose two color measurements differ by more than 0.2 mag.

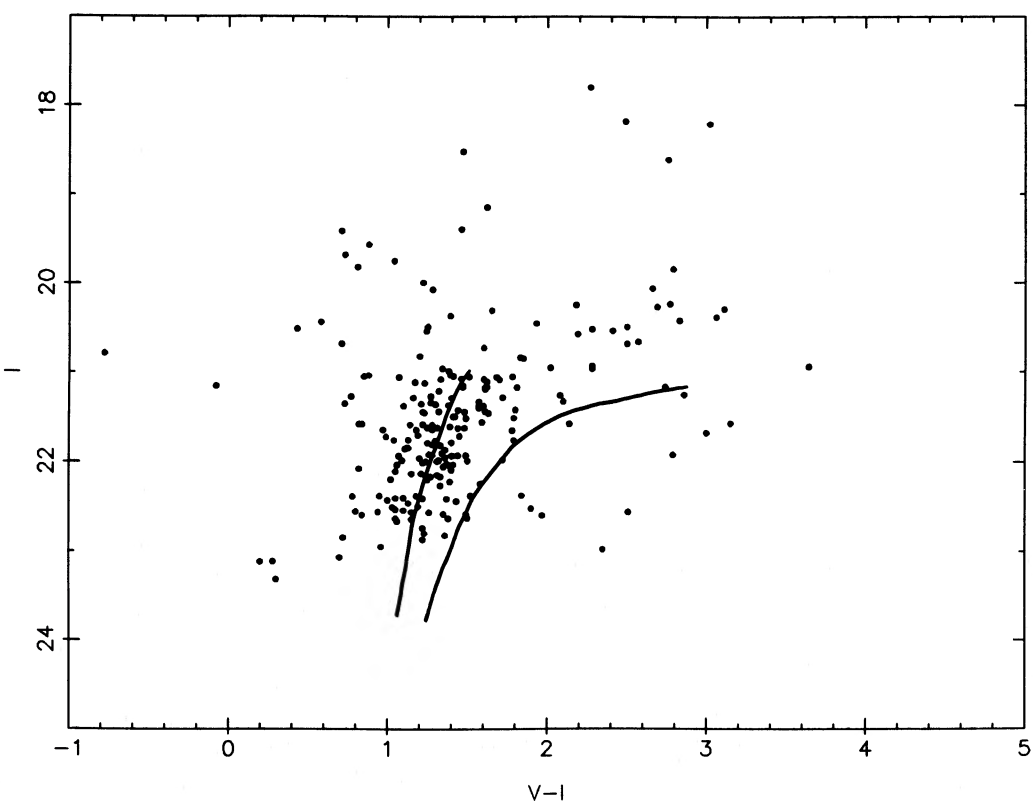

FIG. 4.—Color-magnitude diagram of the M33 halo field. Giant branches for M92 (*blue side*) and 47 Tuc (*red side*) are superposed at the adopted distance and reddening of M33.

and Tammann (1976) with the Paper I Hyades correction. Comparison of the M33 color-magnitude diagram with the giant branches of M92 and 47 Tuc (Fig. 4) indicates that the M33 halo is, first of all, clearly present 7 kpc from the center of the galaxy, and is much more metal-poor on average than the field of similar galactocentric radius in M31. The value of $\langle V - I \rangle$ at $M_I = -3$ is 1.28, but with a large photometric zeropoint uncertainty of 0.10 mag. This implies $\langle [M/H] \rangle = -2.2 \pm 0.8$ in this field. The value of $\sigma(V - I)$ is 0.21, or 0.15 after correction for the estimated photometric errors. Given the error estimate on $\langle V - I \rangle$, it is uncertain at the 1 σ level whether there are any stars in Figure 4 significantly more metal-poor than M92. More accurate photometry is required to decide the issue. What is clear is that the spheroid of M33 contains stars at least as metal-poor as the most metal-poor Galactic globular clusters. We can compare star counts in the M33 field with the predicted surface brightness of the bulge of the galaxy reported by Boulesteix *et al.* (1979). With the parameters determined for their $r^{1/4}$ law bulge, we estimate $3 \times 10^4\ L_{B\odot}$ would be present in our 12 arcmin^2 field. The M92 luminosity function of Hartwick (1970) contains 15 stars in the first V magnitude of the giant branch within an annulus that also, coincidentally, contains $3 \times 10^4\ L_{B\odot}$ (King 1966). We count 36 red giants, in the first V magnitude of the M33 field with $V - I < 2.5$, after correction for 10 presumed foreground stars in the previous 1 mag. This should be regarded as satisfactory agreement, since it is based on a surface brightness extrapolation of three or four orders of magnitude.

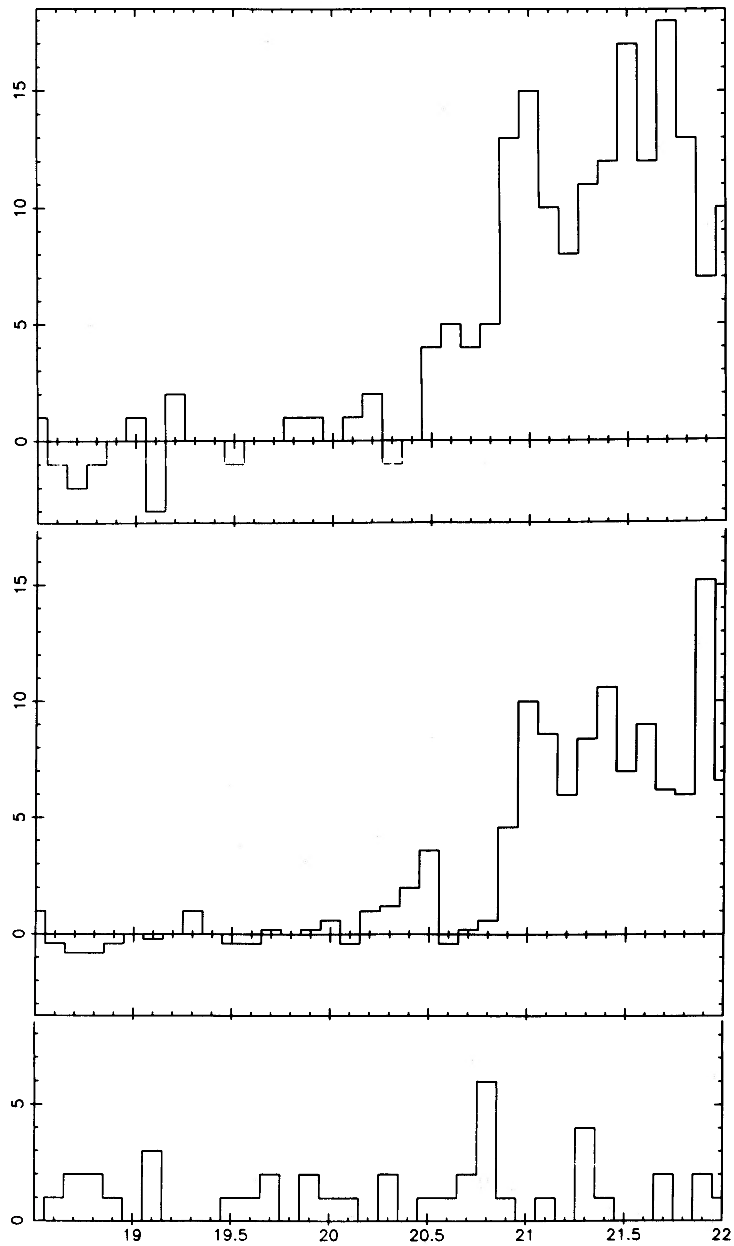

FIG. 5.—Luminosity functions in I magnitudes for M31 (*top*), M33 (*middle*), and the control field from Paper I (*bottom*). The galaxy luminosity functions were corrected for foreground stars using the control field data as described in the text.

IV. THE DISTANCES OF M31 AND M33 FROM THE BRIGHTNESS OF THE TIP OF THEIR GIANT BRANCHES

The brightness of the tip of the red giant branch can be used as a distance indicator. It has been shown by Frogel, Cohen, and Persson (1983) to be in good agreement with theoretical predictions. It appears to be reasonably well defined in Figures 3 and 4. What we are looking for in these figures is a discontinuity in surface density as a function of magnitude, and a visual inspection of Figures 3 and 4 clearly shows such a discontinuity at I of approximately 20.6 and 21.0 respectively.

Figure 5 is an attempt to view the problem in another way. It shows I-magnitude luminosity functions computed from the data in Figures 3 and 4, for $V - I$ in the range 1.0–2.5, corrected for foreground stars. The foreground correction was done by scaling the field luminosity function given in Paper I to the number of stars in the interval $18 < I < 20$. The field luminosity function is shown in the bottom panel of Figure 5; the scaling factors are 1 in M31 and 0.4 in M33. Statistical uncertainties can be estimated from the noise at brighter magnitudes and in the control field. Fluctuations of about four stars in adjacent 0.1 mag bins are typical. For a 2 σ detection of the tip of the giant branch, therefore, we look for an excess of more than eight stars in adjacent bins. This occurs at $I = 20.55$ in M31 and 20.95 in M33, with the uncertainty no larger than 0.15 mag. This procedure is subject to problems of small-number statistics and uncertain selection effects, but it agrees very well with a subjective direct inspection of Figures 3 and 4, from which one would say that the discontinuity certainly occurs between the limits given.

The mean values for $V - I$ at the tip of the giant branches are 1.97 for M31 and 1.60 for M33. Combining these values with the I magnitudes calculated above gives apparent bolometric magnitudes of 20.85 and 21.4 respectively. Equation (4) of Frogel, Cohen, and Persson (1983) predicts absolute bolometric magnitudes of -3.55 ± 0.1 and -3.4. The distance moduli of M31 and M33 on this basis, therefore, are 24.4 ± 0.2 and 24.8 ± 0.2.

Of the two comprehensive extragalactic distance scales in widespread use, the present results are consistent with that of Sandage and Tammann (1976),[1] rather than that of de Vaucouleurs (1978). They are not consistent with recent revisions of the M33 distance by Sandage and Carlson (1983) and Sandage (1983), $[(m - M)_0 = 25.23]$, nor with the result of Madore *et al.* (1985): $[24.25 \pm 0.15]$. These contending revisions are all based on Cepheid photometry. The Population II distance scale is free of some of the problems discussed at length in these papers, such as internal reddening. The location of the red giant tip has been shown to be in excellent agreement with theoretical predictions (Frogel, Cohen, and Persson 1983). Theory suggests very slight dependence on the helium abundance or age of the population, quantities which are unlikely to vary from system to system if standard models are correct.

At the same time we would stress that we are still a long way from being able to offer a mature distance indicator. We need to examine a number of Local Group galaxies of different type, such as the Magellanic Clouds, for example. Larger samples are required in the galaxies we have studied in the M31 neighborhood to reduce the statistical errors. For absolute calibration it is desirable to compare directly with globular clusters observed in the Cousins I system. Even when this is done, this indicator is limited to modest distances, perhaps 10 Mpc with Hubble Space Telescope. But within this volume we suggest the red giant tip may prove a useful link in the extragalactic distance scale.

This work was partially supported by NSF grants AST 83-06139 and AST 85-02518.

[1] Note that the Sandage and Tammann distances, which the present work verifies, have been corrected by 0.26 mag for a subsequent Hyades distance revision. They are the distances adopted by Aaronson, Mould, and Huchra (1980). Indeed, since the distances of M31 and M33 are the cornerstone of the Tully-Fisher relation, the present results constitute support for the lower value of H_0 advocated by Aaronson (1982).

APPENDIX

An anonymous referee has suggested that an alternative digital photometry program should be applied to the data. In particular, the program DAOPHOT (Stetson 1985) was recommended, which fits a point spread function compiled from bright uncontaminated stars to each program star. We have followed this suggestion, locating and carrying out photometry of 1942 stars in the full 800×800 pixels of the M31 field, and 836 stars in the corresponding area of M33. The resultant color-magnitude diagrams shown in Figure 6 contain many more stars because of the use of an automatic star finding algorithm. The advantage of this approach is objectivity; the disadvantage is decreased accuracy due to selection of confused objects for photometry. For 256 stars in common between the DAOPHOT sample and Table 1, we found $\sigma_I = 0.045$ and $\sigma_{V-I} = 0.09$ with no strong dependence on magnitude. For 121 stars in common between the DAOPHOT sample and Table 2 we found $\sigma_I = 0.05$ and $\sigma_{V-I} = 0.07$.

The existence of such small scatter in results from the two different techniques is not surprising. Point spread function photometry is only beneficial in the current application in considerably more confused fields. Our conclusion regarding the width of the M31 halo giant branch is therefore verified by this experiment.

Having a much larger sample of stars in M31 does offer a statistical improvement in the luminosity function. However, the luminosity function for the larger sample still shows a unique step in the bin centered on $I = 20.55$. In M33 the available sample at $I \approx 21$ is only doubled, and the new luminosity function closely resembles that of Figure 5 without significant improvement. So again our conclusions are unchanged by the DAOPHOT experiment.

We thank James Nemec for assistance with the DAOPHOT program and Peter Stetson for making it available.

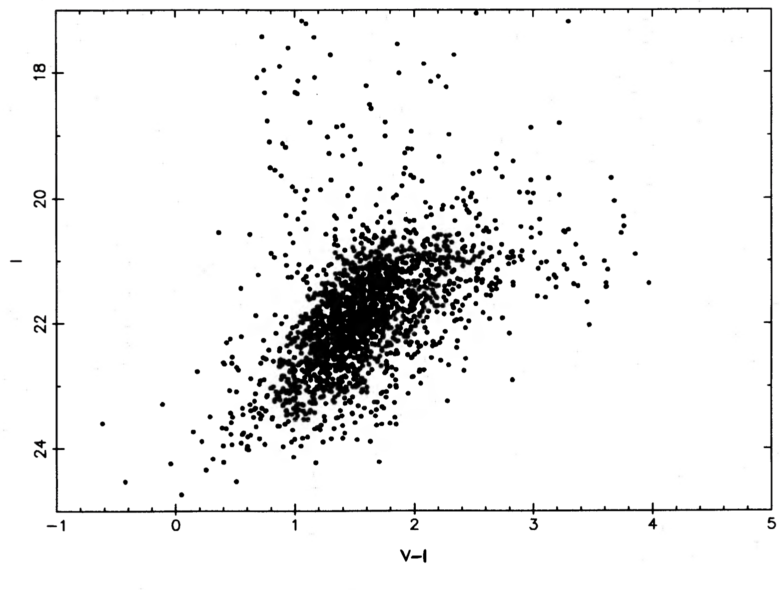

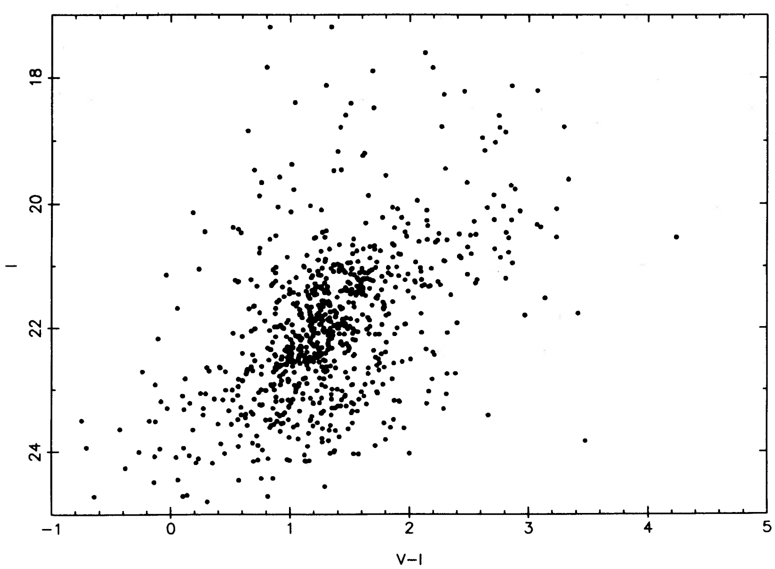

FIG. 6.—Color-magnitude diagrams obtained by application of DAOPHOT. The M31 field is above and the M33 field below

REFERENCES

Aaronson, M. 1982, *Highlights Astr.*, **6**, 267.
Aaronson, M., Mould, J. R., and Huchra, J. P. 1980 *Ap. J.*, **237**, 655.
Baade, W. 1944, *Ap. J.*, **100**, 137.
Boulesteix, J., Colin, J., Athanassoula, E., and Monnet, G. 1979, in *Photometry, Kinematics and Dynamics of Galaxies*, ed. D. S. Evans (Austin: University of Texas, Department of Astronomy), p. 271.
Burstein, D., and Heiles, C. 1984, *Ap. J. Suppl.*, **54**, 33.
Christian, C. A., and Schommer, R. A. 1983, *Ap. J.*, **275**, 92.
Ciardullo, R., and Demarque, P. 1977, *Trans. Astr. Obs. Yale Univ.*, **33**.
Cousins, A. W. J. 1976, *Mem. R.A.S.*, **81**, 25.
Cram, T. R., Roberts, M. S., and Whitehurst, R. N. 1980, *Astr. Ap. Suppl.*, **40**, 215.
de Vaucouleurs, G. 1958, *Ap. J.*, **128**, 465.
———. 1959, *Ap. J.*, **130**, 728.
———. 1978, *Ap. J.*, **223**, 730.
Freeman, K. C. 1970, *Ap. J.*, **160**, 811.
Frogel, J. A., Cohen, J. G., and Persson, S. E. 1983, *Ap. J.*, **275**, 773.
Gunn, J. E., and Westphal, J. A. 1981, *Proc. SPIE*, **290**, 16.
Hartwick, F. D. A. 1970, *Ap. J.*, **161**, 845.
Hodge, P. W. 1981, *Atlas of the Andromeda Galaxy* (Seattle: University of Washington Press).
King, I. 1966, *A.J.*, **71**, 276.
Madore, B. F., McAlary, C. W., McLaren, R. A., Welch, D. L., Neugebauer, G., and Matthews, K. 1985, *Ap. J.*, **294**, 560.
Mould, J. R. 1984, *Pub. A.S.P.*, **96**, 773.
Mould, J. R., and Aaronson, M. 1983, *Ap. J.*, **273**, 530.
Mould, J. R., Kristian, J., and Da Costa, G. S. 1983, *Ap. J.*, **270**, 471 (Paper I).
———. 1984, *Ap. J.*, **278**, 575 (Paper II).
Newton, K. 1980, *M.N.R.A.S.*, **190**, 689.
Sandage, A. R. 1983, *A.J.*, **88**, 1108.

Sandage, A. R., and Carlson, G. 1983, *Ap. J.* (*Letters*), **267**, L25.
Sandage, A. R., and Tammann, G. 1976, *Ap. J.*, **210**, 7.
Sargent, W. L. W., Kowal, C., Hodge, P. W., and van den Bergh, S. 1977. *A.J.*, **82**, 947.
Stetson, P. 1985, *DAOPHOT Users Manual.*
van den Bergh, S. 1968, *Comm. David Dunlap Obs.*, No. 195.
van der Kruit, P., and Searle, L. 1983, *Astr. Ap.*, **110**, 79.

JEROME KRISTIAN: Mount Wilson and Las Campanas Observatories, 813 Santa Barbara Street, Pasadena, CA 91101

JEREMY MOULD: Department of Astronomy, California Institute of Technology, Pasadena, CA 91125